Ceramics International **24** (1998) 117–124

PII: S0272-8842(97)00040-0
0272-8842/97 $17.00+.00

Morphological Characteristics of Low Density and High Lithium Content $Li_xNi_{1-x}O$ Cathodes for Molten Carbonate Fuel Cells

E. Antolini & L. Giorgi

ENEA C.R.E. Casaccia, Erg Tea Echi, Via Anguillarese 301, 00060 Santa Maria di Galeria, Rome, Italy

(Received 10 February 1997; accepted 21 April 1997)

Abstract: $Li_xNi_{1-x}O$ cathode structures were prepared by solid state reaction in air of nickel and lithium carbonate powder mixtures. Density changes of Ni/Li_2CO_3 composites following thermal treatment at 700°C were determined as a function of starting composition and isothermal time so as to evaluate the effect of Li_2CO_3 content in the starting mixture on the microstructure of the resulting $Li_xNi_{1-x}O$ solid solutions. Total porosity, calculated from density data, increased up to the composition with 23 at% Li+, beyond which the porosity was nearly constant. An analysis of the compositions with nominal 30 and 44 at% Li+ showed that, by Li_2CO_3 decomposition during isothermal treatment at 700°C, both the amount and lithium atomic fraction of $Li_xNi_{1-x}O$ solid solution increased with time, but the porosity of the solid solution was unchanged. It was denoted that lithium carbonate affects lithium nickel oxide porosity by mass-to-void transformation during the reaction of Li_2CO_3 with $Li_yNi_{1-y}O$ to get $Li_xNi_{1-x}O$ with $x > y$, and by carbon oxide and/or carbon dioxide evolution following Li_2CO_3 decomposition. While the specific pore volume related to mass-to-void transformation increased with Li_2CO_3 amount, for high lithium content solid solutions, the specific pore volume, due to gas evolution, decreased with lithium carbonate content of the mixture. © 1997 Elsevier Science Limited and Techna S.r.l.

1 NOTATION

a	Lattice constant of cubic rock salt solid solution
$a_{h,c}$	Lattice constants of hexagonal solid solution
A_L	Undecomposed to total lithium carbonate mass ratio
M_h	Lithium nickel oxide molecular weight with $x = x_h$
M_l	Lithium nickel oxide molecular weight with $x = x_l$
M_L	Lithium atomic weight
$M_{Li<x>Ni1-<x>O}$	Lithium nickel oxide molecular weight with $x = <x>$
$M_{Li_xNi_{1-x}O}$	Lithium nickel oxide molecular weight at the end of thermal treatment
$M_{Li_yNi_{1-y}O}$	Lithium nickel oxide molecular weight after 0.5 h isothermal treatment
$M_{Li_2CO_3}$	Lithium carbonate molecular weight
M_N	Nickel atomic weight
M_O	Oxygen atomic weight
P	Total porosity
P^e	Total porosity at the end of thermal treatment
$P_{Ni_xNi_{1-x}O}$	Total porosity of lithium nickel oxide
P^o	Total porosity after 0.5 h of isothermal treatment
PWC_e	Plaque weight change at the end of the isothermal treatment
PWC_t	Plaque weight change after t time of isothermal treatment
PWC^*	Calculated plaque weight change in the absence of Li_2CO_3 decomposition.
$V_{Li_xNi_{1-x}O}$	Lithium nickel oxide volume per plaque unit mass
$V_{Li_xNi_{1-x}O^e}$	Lithium nickel oxide volume per starting plaque ($t = 0.5$ h) unit mass at the end of thermal treatment
$V_{Li_xNi_{1-x}O^o}$	Lithium nickel oxide volume per unit mass of the starting mixture ($t = 0.5$ h) after 0.5 h of isothermal treatment
$V_{Li_2CO_3}$	Lithium carbonate volume per plaque unit mass

$V_{Li_2CO_3}^{o}$	Lithium carbonate volume per plaque unit mass after 0.5 h of isothermal treatment
V_{tot}^{e}	Total volume per unit mass of the starting mixture ($t=0.5$ h) at the end of thermal treatment
V_{tot}^{o}	Specific volume of the $Li_xNi_{1-x}O/Li_2CO_3$ composite after 0.5 h of isothermal treatment
V_v	Specific pore volume
V_v^{e}	Pore volume per unit mass of the starting mixture ($t=0.5$ h) at the end of thermal treatment
V_v^{g}	Gas evolution pore volume per unit mass of starting mixture ($t=0.5$ h) at the end of thermal treatment
$V_v^{Li_xNi_{1-x}O}$	$Li_xNi_{1-x}O$ pore volume per plaque unit mass
$V_v^{Li_2CO_3}$	Li_2CO_3 pore volume per plaque unit mass
V_v^{o}	Specific pore volume after 0.5 h of isothermal treatment
V_v^{*}	Mass-to-void transformation pore volume per unit mass of starting mixture ($t=0.5$ h) at the end of thermal treatment
$W_{Li_xNi_{1-x}O}^{e}$	Mass of $Li_xNi_{1-x}O$ at the end of thermal treatment
$<x>$	Average lithium atomic fraction of lithium nickel oxide
x_h	Lithium atomic fraction of higher Lithium content solid solution
x_l	Lithium atomic fraction of lower lithium content solid solution
x_n	Nominal lithium atomic fraction
$X_{Li_xNi_{1-x}O}$	Molar fraction of lithium nickel oxide in the $Li_xNi_{1-x}O/Li_2CO_3$ plaque
$X_{Li_2CO_3}$	Mass fraction of lithium carbonate in the $Li_xNi_{1-x}O/Li_2CO_3$ plaque
y_h	Molar fraction of higher lithium content solid solution
Y_h	Mass fraction of higher lithium content solid solution
ρ_h	Theoretical density of higher lithium content solid solution
ρ_l	Theoretical density of lower lithium content solid solution
ρ_s	Experimental density
ρ_{th} (cub)	Theoretical density of lithium nickel oxide in the cubic form
ρ_{th} (hex)	Theoretical density of lithium nickel oxide in the hexagonal form
r_{th}^{lh}	Theoretical density of mixed solid solutions
$\rho_{th}^{Li_xNi_{1-x}O}$	Theoretical density of lithium nickel oxide
$\rho_{th}^{Li_2CO_3}$	Theoretical density of lithium carbonate ($2.11\ g\,cm^{-3}$)
$\rho_{th}^{LN/LC}$	Theoretical density of $Li_xNi_{1-x}O/Li_2CO_3$ mixture
$\rho_{th}^{<x>}$	Theoretical density of lithium nickel oxide with $x=<x>$

2 INTRODUCTION

The cathode structure was recognized early as one of the principal factors determining molten carbonate fuel cell (MCFC) performance. The electrode design ideally has a broad pore size spectrum, which provide small pores for the electrochemical reaction and large pores for gas diffusion.[1] The cathode material must fulfil many requirements: good electronic conductivity, thermal stability at 650°C, chemical stability in the molten carbonate, to be resistant to sintering, swelling, creep and failure in work conditions. Lithiated nickel oxide ($Li_xNi_{1-x}O$) with low lithium content ($0.02<x<0.05$) met these requirements, but its dissolution in molten carbonates electrolyte under cell operating conditions is one of the most important problems concerning MCFC development.[2] A recent work showed that $Li_xNi_{1-x}O$ with high lithium content ($x<0.2$) has a relatively lower rate of solubility than $Li_xNi_{1-x}O$ with low Li+ content and that the change in lithium content in $Li_xNi_{1-x}O$ is very slow in molten carbonate.[3] On this basis our attention is focused on $Li_xNi_{1-x}O$ with high lithium content as an improved cathode material. High lithium content $Li_xNi_{1-x}O$ can be obtained only by out-of-cell nickel oxidation and lithiation (by in-cell lithiation only low lithium content $Li_xNi_{1-x}O$ can be obtained).[4] Out-of-cell $Li_xNi_{1-x}O$ can be obtained by solid state reaction of nickel and lithium carbonate.[5] In addition to serving as lithium source, lithium carbonate acts as pore former:[6,7] Li_2CO_3 presence in the starting mixture gives rise to the formation of micropores. A previous work deals on the effect of the thermal treatment at $T\geq900$°C of Ni/Li_2CO_3 mixtures on the microstructure of the resulting $Li_xNi_{1-x}O$:[7] at these temperatures sintering processes in the samples with high lithium content are present, due both lithium oxide evaporation[8] and liquid phase sintering (Li_2CO_3 melts at 723°C).[9] To aim to study the microstructure of high lithium content $Li_xNi_{1-x}O$ in the absence of sintering process, in the present work particular attention was focused on thermal treatment at 700°C of two high lithium content compositions (30 and 44 at%), to avoid lithium loss[10] and sintering processes. As by Hg-porosity measurements it is not possible to evaluate the microporosity of these structures,[7] the porosity was calculated by density data.

3 EXPERIMENTAL

Nickel INCO 255 and lithium carbonate Merck 5671 powders were used as starting materials. Mixtures of these powders (with lithium atomic fraction in the range 0.00–0.44) were ball milled with a binder, an antifoam agent and deionized water. The resulting slurries were degassed and then cast on to bee's wax coated glass surface. After the tapes were dried and disc-shaped samples

(diameter 5 cm) were cut from them. The thickness of the samples was 0.050 cm. The specimens were put on porous alumina platform and were treated at 700, 750, 800 and 900°C, according to the following thermal cycle:

(i) heating at 3.6°C min^{-1} from room temperature to the processing temperature;

(ii) isothermal holding for times in the range 0–20 h;

(iii) cooling at 1.8°C min^{-1} to room temperature.

Thermal treatments were performed in air using a BICASA BE 35 furnace. The plaque diameter and thickness were measured before and after thermal treatment by a digital caliper (Facom No. 1742.1). The overall precision of the measurements was $\pm 10^{-3}$ cm.

X-ray diffraction measurements were performed using a Philips PW1710 powder diffractometer equipped with a Philips PW1050 vertical goniometer using CuK_α radiation. Density measurements were obtained by two ways: (1) mass/volume measurements and (2) Archimedes' method in mercury.

Table 1. Lattice constants of $Li_xNi_{1-x}O$ solid solutions following thermal treatment at 700°C up to reaching a constant weight

X_{li} (at%)	700°C Lattice constant (Å)		Structure	x (at%)
0	a 4.1735		Cub	0
6	a_1 4.1671		Cub1	4
	a_2 4.1570		Cub2	10
12	a_1 4.1672		Cub1	4
	a_2 4.1463		Cub2	16
23	a_1 4.1680		Cub1	4
	a_2 4.1270		Cub2	27
30	a_1 4.1688	*	Cub1	3
	a_2 4.1330	*	Cub2	22
	a_1 4.1379		Cub1	19
	a_2 4.1114		Cub2	33
44	a_1 4.1672	*	Cub1	4
	a_2 4.1269	*	Cub2	25
	a 4.0921		Cub	43
	a_h 2.8898		Hex	43
	c 14.2120			

Cub1: lower-lithium-content phase; Cub2: higher-lithium-content phase.
*Data obtained following 0.5 h of thermal treatment at 700°C.

4 RESULTS AND DISCUSSION

The resulting cathode structures were brittle and must be assembled in cell with care, to avoid possible breakage. During the thermal treatment of the mixtures, the following processes occurred: nickel oxidation, burn-out of organic compounds, lithium carbonate decomposition and lithium nickel oxide formation. All but 0 and 6 at% Li+ compositions showed plaque dilatation for all thermal treatment times at 700°C.

Table 1 shows $Li_xNi_{1-x}O$ lattice constants obtained from X-ray diffraction measurements following thermal treatments of Ni/Li_2CO_3 mixtures at 700°C in air up to reaching a constant weight. Following thermal treatment at 700°C, we can denote the presence of two solid solutions, one with lattice constant higher, and another with lattice constant lower than that related to nominal lithium content.[11,12] We have calculated theoretical density of these compositions in the following way:

(i) first, we have calculated x_h and x_l by the dependence of $Li_xNi_{1-x}O$ lattice parameter on lithium atomic fraction, true up to $x=0.20$, as reported in Ref. 11, and for $x>0.20$ by the dependence of $Li_xNi_{1-x}O$ unit cell volume on lithium atomic fraction, as reported in Ref. 12.

(ii) From the value of nominal and experimental lithium atomic fraction values, we have calculated the molar fraction of the solid solution with higher lithium content, as:

$$y_h = (x_n - x_l)/(x_h - x_l) \quad (1)$$

The molar fraction is related to mass fraction by:

$$Y_h = y_h/[y_h + (1 - y_h)M_l/M_h] \quad (2)$$

(iii) then we have evaluated theoretical density of the solid solutions as the following equations for cubic rock salt and hexagonal crystal structure (only for 44 at% Li+), respectively:

$$\rho_{th}(\text{cub}) = 4[M_O + (1 - x)M_N + xM_L]/a^3 \quad (3)$$

$$\rho_{th}(\text{hex}) = 6[M_O + (1 - x)M_N + xM_L]/0.866a_h^2c \quad (4)$$

(iv) finally, we have calculated theoretical density of the mixture of two solid solutions as:

$$\rho_{th}^{lh} = \rho_{th}^h\rho_{th}^l/[Y_h\rho_{th}^l + (1 - Y_h)\rho_{th}^h] \quad (5)$$

Figure 1 shows the dependence of theoretical density on nominal lithium atomic fraction x of $Li_xNi_{1-x}O$ solid solution. The values of experimental and theoretical densities are reported in Table 2. Density values obtained by mass/volume measurements were in agreement with picnometer measurements. From density values of Table 2 we have calculated total porosity of the solid solution by the relation:

$$P = 1 - \rho_s/\rho_{th}^{lh} \quad (6)$$

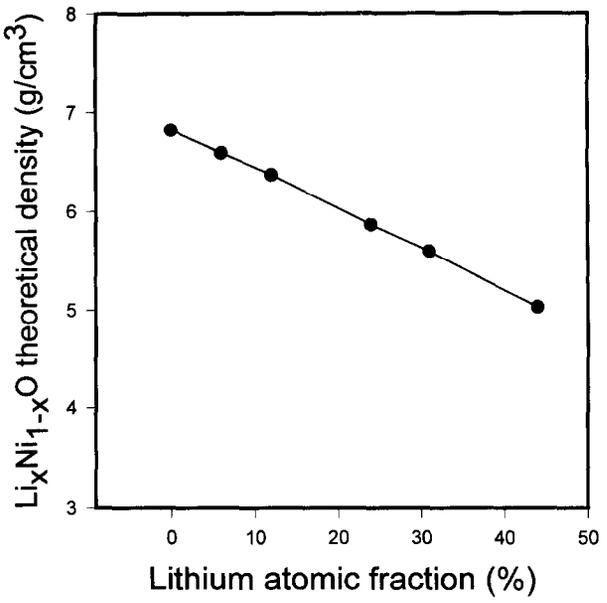

Fig. 1. Dependence of $Li_xNi_{1-x}O$ theoretical density on lithium atomic fraction ot the solid solution.

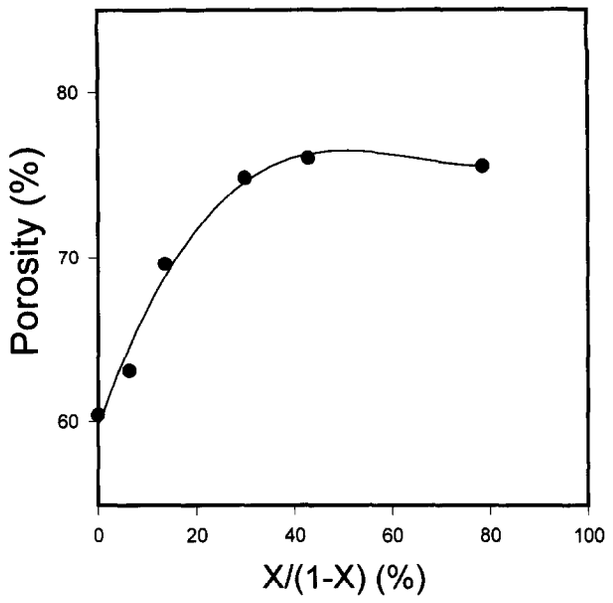

Fig. 2. Relation between total porosity, calculated from density measurements, and Li/Ni atomic ratio ($x/(1-x)$).

As shown in Fig. 2, where plaque porosity after thermal treatment at 700°C is plotted against Li/Ni atomic ratio ($x/(1-x)$), the porosity increased up to 23 at% Li+, above it was nearly constant. In the absence of sintering processes, the parameters affecting $Li_xNi_{1-x}O$ porosity can be separed in two groups: (i) parameters independent of Li_2CO_3 presence, and (ii) parameters related to the presence of Li_2CO_3 in the starting mixture. Starting nickel particle porosity, nickel oxidation and the presence and burn-out of organic compound are referred to the former group; mass-to-void transformation during the reaction of Li_2CO_3 with $Li_yNi_{1-y}O$ to get $Li_xNi_{1-x}O$ (with $x > y$), and carbon oxide and/or carbon dioxide evolution from the plaque by lithium carbonate decomposition are to be inserted in the latter group.

To better understand the way of formation of $Li_xNi_{1-x}O$ microstructure following Li_2CO_3 decomposition, we have evaluate time dependence of porosity of two compositions with high lithium content, 30 and 44 at% Li+. As shown in Fig. 3, total porosity of these two compositions, obtained from density values, strongly decreased with thermal treatment temperature, essentially by reactive liquid phase sintering. From X-ray diffracton measurements it was denoted that, after 0.5 h of thermal treatment at 700°C, the plaque was constituted by $Li_xNi_{1-x}O$ and Li_2CO_3 phases. As shown in Table 1, going from 0.5 to the end of isothermal treatment, the values of lattice constant were shifted towards higher lithium contents. We have calculated the amount of undecomposed Li_2CO_3 for different times of isothermal treatment as the following relation:

$$A_L = [PWC_t - PWC_e]/[PWC^* - PWC_e] \quad (7)$$

Table 2. Experimental $Li_xNi_{1-x}O$ densities following thermal treatment at 700°C of various Ni/Li_2CO_3 mixtures up to constant weight, and theoretical $Li_xNi_{1-x}O$ densities, calculated from eqn (5)

X_{Li} (at%)	Experimental density (g cm^{-3})	Theoretical density (g cm^{-3})
0	2.70	6.82
6	2.43	6.59
12	1.93	6.35
23	1.53	5.90
30	1.36	5.60
44	1.25	5.08

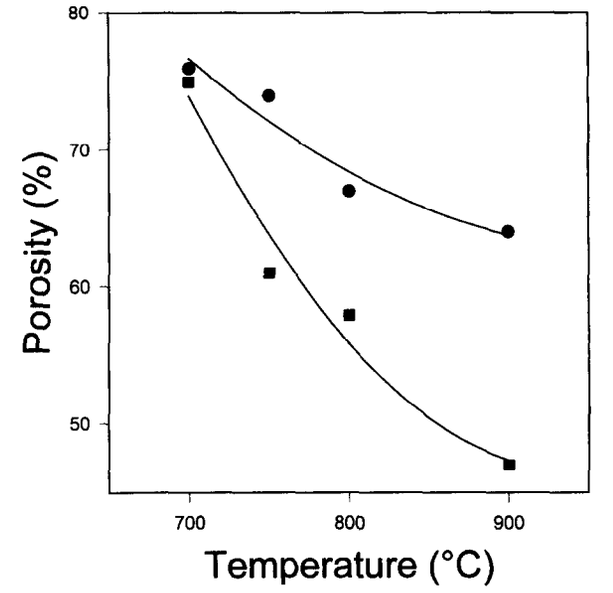

Fig. 3. Total porosity as a function of temperature for (●) 30 and (■) 44 at% Li+ compositions.

From A_L values we have determined the average lithium atomic fraction for different times of isothermal treatment $< x >$:

$$< x >= x_n(1 - A_L)/[1 - x_n A_L] \tag{8}$$

By using A_L and $< x >$, it is possible to determine Li_2CO_3 mass fraction $X_{Li_2CO_3}$ in the plaque following various thermal treatments:

$$X_{Li_2CO_3} = x_n M_{Li_2CO_3} A_L/[2(1- < x >)(1 - x_n) \\ M_{Li<x>Ni1-<x>O} + x_n M_{Li_2CO_3} A_L] \tag{9}$$

Theoretical density of $Li_{<x>}Ni_{1-<x>}O/Li_2CO_3$ plaque after different times of isothermal treatment was calculated as:

$$\rho_{th}^{LN/LC} = \rho_{th}^{<x>} \rho_{Li_2CO_3}/[X_{Li_2CO_3}\rho_{th}^{<x>} \\ + (1 - X_{Li_2CO_3})\rho_{Li_2CO_3}] \tag{10}$$

Finally, lithium nickel oxide molar fraction in the $Li_xNi_{1-x}O/Li_2CO_3$ plaque was determined as:

$$X_{Li_{<x>}Ni_{1-<x>}O} = (1 - X_{Li_2CO_3})/[1 - X_{Li_2CO_3} \\ \left(1 - M_{Li_{<x>}Ni_{1-<x>}O/M_{Li_2CO_3}}\right)] \tag{11}$$

Figures 4 and 5 show time dependence at 700°C of $< x >$ and $Li_xNi_{1-x}O$ molar fraction for 30 and 44 at% Li+: $< x >$ and $Li_xNi_{1-x}O$ amount increased with thermal treatment up to the disappearance of all lithium carbonate. Tables 3 and 4 show the values of experimental and theoretical densities of $Li_{<x>}Ni_{1-<x>}O/Li_2CO_3$ mixtures, as well as the values of PWC_t, A_L, $M_{Li_{<x>}Ni_{1-<x>}O}$ and $X_{Li_2CO_3}$. Using these values, from the following relation:

$$P = 1 - \rho_s/r_{th}^{LN/LC} \tag{12}$$

we have calculated the porosity of $Li_{<x>}Ni_{1-<x>}O/Li_2CO_3$ plaque. Figure 6 shows the dependence of total porosity on isothermal treatment time: the upper line is related to sample with 30 at% Li+, the lower line is due to the composition with 44 at% Li+. Plotting total porosity vs $Li_xNi_{1-x}O$ molar fraction, instead, only one line for both 30 and 44 at% samples was obtained, as shown in Fig. 7.

In the hypothesis that specific pore volume of Li_2CO_3 is zero, we have calculated lithium nickel oxide porosity $P_{Li_xNi_{1-x}O}$ for different isothermal times. Total porosity can be written as:

$$P = V_v/(V_v + V_{Li_xNi_{1-x}O} + V_{Li_2CO_3}) \tag{13}$$

The specific pore volume and the porosity of lithium nickel oxide are given by:

$$V_v = V_v^{Li_xNi_{1-x}O} + V_v^{Li_2CO_3} \tag{14}$$

$$P_{Li_xNi_{1-x}O} = V_v^{Li_xNi_{1-x}O}/(V_v^{Li_xNi_{1-x}O} + V_{Li_xNi_{1-x}O}) \tag{15}$$

In the hypothesis that $V_v^{Li_2CO_3=0}$, from eqns (13)–(15) one obtains:

$$P_{Li_xNi_{1-x}O} = P/(1 - PV_{Li_2CO_3}/V_v) \tag{16}$$

Table 3. Plaque weight change (PWC_t), undecomposed Li_2CO_3 (A_L), molecular weight of the solid solution, Li_2CO_3 mass fraction, experimental density and theoretical density (as the eqn (10)) for different isothermal times at 700°C for samples with nominal x_{Li} 0.30

Time (h)	PWC_t (wt%)	A_L (wt%)	$M_{Li_{<x>}Ni_{1-<x>}O}$ (g)	$X_{Li_2CO_3}$ (wt%)	Experimental density ($g\,cm^{-3}$)	Theoretical density ($g\,cm^{-3}$)
0.5	11	63	67.46	14.6	1.65	4.86
5	8.4	28	62.29	8.6	1.39	5.11
10	6.3	0	59.18	0.0	1.36	5.59

Table 4. Plaque weight change (PWC_t), undecomposed Li_2CO_3 (A_L), molecular weight of the solid solution, Li_2CO_3 mass fraction, experimental density and theoretical density (as the eqn (10)) for different isothermal times at 700°C for samples with nominal x_{Li} 0.44

Time (h)	PWC_t (wt%)	A_L (wt%)	$M_{Li_{<x>}Ni_{1-<x>}O}$ (g)	$X_{Li_2CO_3}$ (wt%)	Experimental density ($g\,cm^{-3}$)	Theoretical density ($g\,cm^{-3}$)
0.5	6.3	68	64.35	28	1.67	3.96
5	2.1	32	56.59	20	1.36	4.11
10	0.0	15	54.01	12	1.34	4.42
20	−1.7	0	51.93	0	1.25	5.03

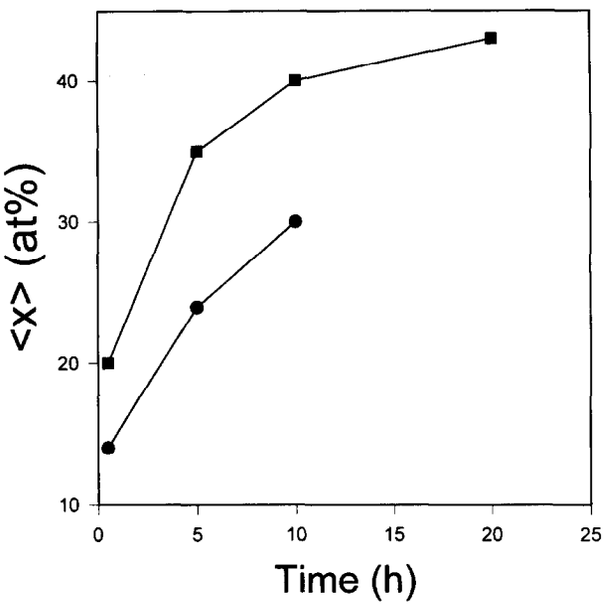

Fig. 4. Time dependence at 700°C of average lithium atomic fraction $<x>$ in lithium nickel oxide solid solution. (●) 30 at% Li+ sample; (■) 44 at% Li+ sample.

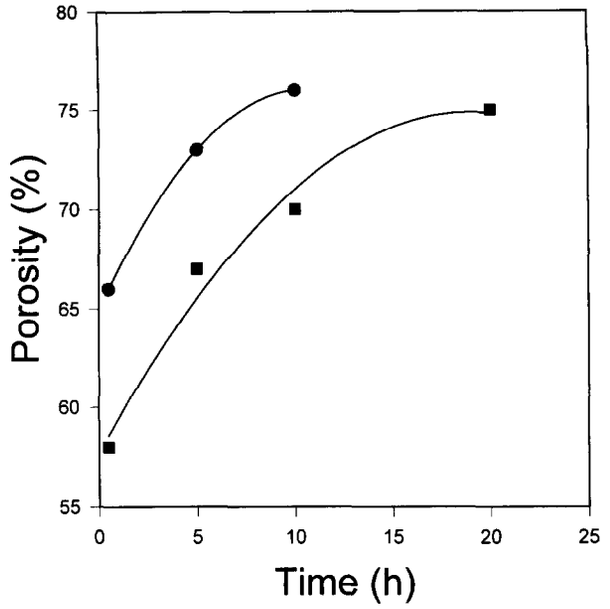

Fig. 6. Total porosity of $Li_xNi_{1-x}O/Li_2CO_3$ plaques as a function of thermal treatment time. (●) 30 at% Li+ sample; (■) 44 at% Li+ sample.

Being, from the relation (13):

$$V_v = (V_{Li_xNi_{1-x}O} + V_{Li_2CO_3})P/(1-P). \quad (17)$$

and being the volume of Li_2CO_3 and $Li_xNi_{1-x}O$ per unit mass of the plaque:

$$V_{Li_2CO_3} = X_{Li_2CO_3}/\rho_{Li_2CO_3} \quad (18)$$

$$V_{Li_xNi_{1-x}O} = (1 - X_{Li_2CO_3})/\rho_{Li_xNi_{1-x}O} \quad (19)$$

we have calculated $P_{Li_xNi_{1-x}O}$. Figure 8 shows the dependence of lithium nickel oxide porosity on $Li_xNi_{1-x}O$ atomic fraction: lithium nickel oxide porosity was nearly independent on the amount of $Li_xNi_{1-x}O$. On this basis, from the following relationship, with $V_v^{Li_2CO_3} = 0$ and $P_{Li_xNi_{1-x}O} = 0.755$, we have calculated the plaque porosity:

$$P = X_{Li_xNi_{1-x}O}P_{Li_xNi_{1-x}O}/[K + X_{Li_xNi_{1-x}O}(1-K)] \quad (20)$$

where $K = M_{Li_2CO_3}\ \rho_{Li_xNi_{1-x}O}\ (1 - P_{Li_xNi_{1-x}O})/(M_{Li_xNi_{1-x}O}\ \rho_{Li_2CO_3})$. The resulting values of porosity were in good agreement with porosity values obtained from eqn (12), as indicated in Table 5.

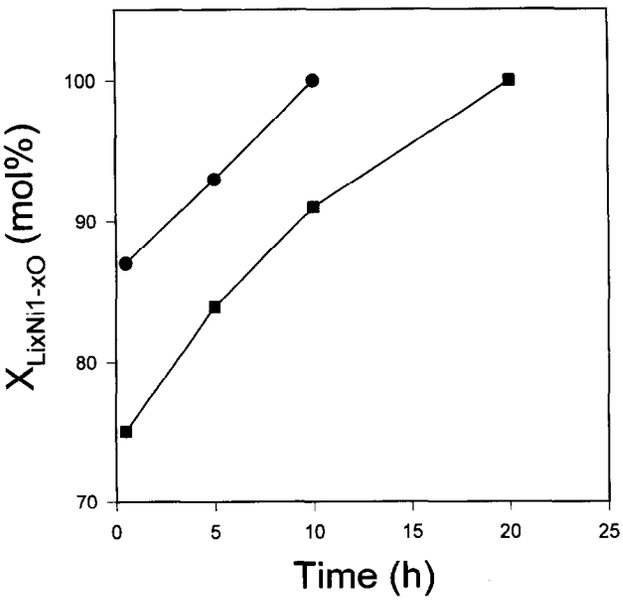

Fig. 5. Time dependence at 700°C of lithium nickel oxide molar fraction in $Li_xNi_{1-x}O/Li_2CO_3$. (●) 30 at% Li+ sample; (■) 44 at%Li+ sample.

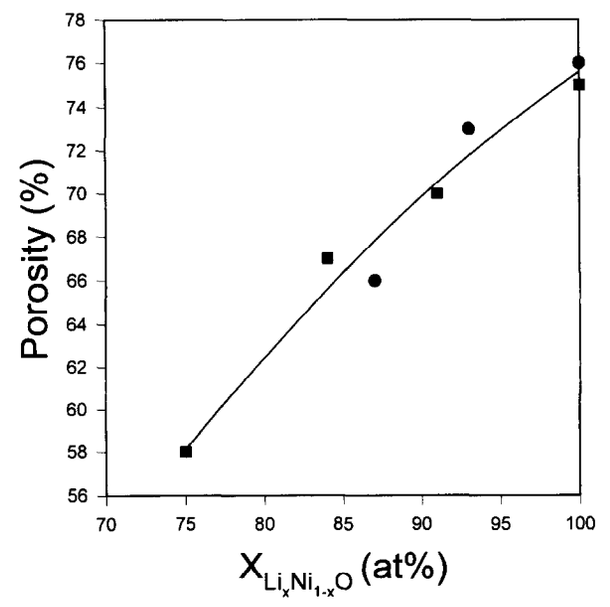

Fig. 7. Total porosity of $Li_xNi_{1-x}O/Li_2CO_3$ plaques as a function of $Li_xNi_{1-x}O$ molar fraction. (●) 30 at% Li+ sample; (■) 44 at% Li+ sample.

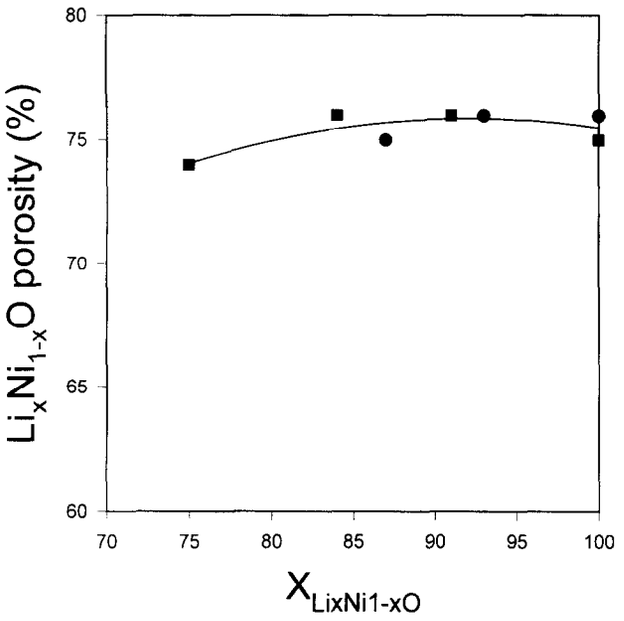

Fig. 8. $Li_xNi_{1-x}O$ porosity of plaques as a function of $Li_xNi_{1-x}O$ molar fraction for (●) 30 and (■) 44 at% Li+ compositions.

Total pore volume at the end of isothermal treatment V_v^e is constituted by the pore volume after 0.5 h of isothermal treatment V_v^o, which depends on starting nickel particle porosity, on nickel oxidation, on the presence and burn-out of organic compounds, and on lithium nickel oxide formed during the dynamic step of thermal treatment and after 0.5 h of isothermal treatment at 700°C, the pore volume due to mass-to-void transformation V_v*, and specific pore volume due to gas evolution (carbon oxide and/or carbon dioxide) by Li_2CO_3 decomposition, as:

$$V_v^e = V_v^o + V_v^* + V_v^g \tag{21}$$

$$V_v^* = V_{Li_2CO_3} + V_{Li_xNi_{1-x}O^o} - V_{Li_xNi_{1-x}O^e} \tag{22}$$

Now we calculate the contribute of mass-to-void transformation and gas evolution to total pore volume at the end of thermal treatment. After 0.5 h of isothermal treatment the specific total volume of $Li_xNi_{1-x}O/Li_2CO_3$ composite is:

$$V_{tot}^o = V_{Li_2CO_3} + V_{Li_xNi_{1-x}O^o} + V_v^o \tag{23}$$

V_v^o is related to porosity by:

$$V_v^o = (V_{Li_xNi_{1-x}O^o} + V_{Li_2CO_3})P^o/(1 - P^o) \tag{24}$$

where P^o is the porosity after $t = 0.5$ h of isothermal treatment.

At the end of reaction (10 h for 30%, 20 h for 44%) one obtains:

$$V_{tot}^e = V_{Li_xNi_{1-x}O^e} + V_v^e \tag{25}$$

$V_{Li_xNi_{1-x}O^e}$ can be written as:

$$V_{Li_xNi_{1-x}O^e} = W_{Li_xNi_{1-x}O^e}/\rho_{Li_xNi_{1-x}O^e} \tag{26}$$

To calculate $W_{Li_xNi_{1-x}O^e}$, starting from the reaction:

$$Li_yNi_{1-y}O + (x - y)/(1 - x)LiO \text{ — > } (1 - y)/(1 - x)\ Li_xNi_{1-x}O \tag{27}$$

being:

$$\text{mol } Li_xNi_{1-x}O = (1 - y)/(1 - x) \text{ mol } Li_yNi_{1-y}O \tag{28}$$

$W_{Li_xNi_{1-x}O^e}$ can be expressed as:

$$W_{Li_xNi_{1-x}O^e} = (1 - y)M_{Li_xNi_{1-x}O}(1 - X_{Li_2CO_3})/(1 - x)\ M_{Li_yNi_{1-y}O} \tag{29}$$

By the relation (25) we can calculate $V_{Li_xNi_{1-x}O^e}$. Knowing $V_{Li_xNi_{1-x}O^o}$ and $V_{Li_xNi_{1-x}O^e}$ it is possible to obtain V_v, V_v^* and V_v^g:

$$V_v = V_{Li_xNi_{1-x}O^e}\ P^e/(1 - P^e) \tag{30}$$

$$V_v^g = V_v - V_v^* - V_v^o \tag{31}$$

Table 5. Porosity values calculated from eqn (6) and from eqn (19) at various $Li_xNi_{1-x}O$ atomic fractions in the plaque for 30 and 44 at% Li+

Nominal Li+ (at%)	$X_{Li_xNi_{1-x}O}$ (at%)	P (from eqn (6)) (%)	P (from eqn (19)) (%)
30	87	66	67
	93	73	71
	1	76	75.5
44	75	58	60
	84	67	65
	91	70	70
	1	75	75.5

Table 6 shows the values of these parameters: for 30 at% Li+ sample $V_v^g > V_v*$, while for 44 at% Li+ composition $V_v* > V_v^g$; moreover, V_v^g for 30 at% Li+ composition was higher than that of 44 at% Li+ sample. For high lithium carbonate content V_v^g decreases with Li_2CO_3 amount: as higher is V_v* as higher is the probability that the gas escapes from the plaque, without the formation of microvoids. The increase of V_v* and the decrease of V_v^g

Table 6. Lithium carbonate and lithium nickel oxide volumes after 0.5 h of isothermal treatment, lithium nickel oxide volume at the end of thermal treatment, mass-to-void pore volume, gas evolution pore volume, and mass-to-void (gas evolution) pore volume to sum of mass-to-void and gas evolution pore volume ratio for 30 and 44 at% compositions

**	Nominal Li+ 30 at%	Nominal Li+ 44 at%
$V_{Li_2CO_3}$ (t=0.5 h) ($cm^3 g^{-1}$)	0.069	0.133
$V_{Li_xNi_{1-x}O}$ (t=0.5 h) ($cm^3 g^{-1}$)	0.136	0.120
$V_{Li_xNi_{1-x}O}$ (t max) ($cm^3 g^{-1}$)	0.165	0.165
V_v^* ($cm^3 g^{-1}$)	0.040	0.088
V_v^g ($cm^3 g^{-1}$)	0.086	0.058
$V_v^*/(V_v^*+V_v^g)$ (%)	32	60
$V_v^g/(V_v^*+V_v^g)$ (%)	68	40

**For all the values the volume is referred to mass unit of mixture after 0.5 h of isothermal treatment.

with Li_2CO_3 content of the mixture can explain the constant porosity value at high lithium content. At low lithium content V_v* is negligible so V_v^g (and P) increases with lithium carbonate amount.

5 CONCLUSIONS

Following thermal treatment at 700°C, total porosity of lithium nickel oxide obtained by solid state reaction of nickel and lithium carbonate powder increased up to 23 at% Li+, above it was nearly constant. Total porosity depends on starting nickel particle porosity, on nickel oxidation, on the presence and burn-out of organic compounds, on mass-to-void transformation related to volume difference between Li_2CO_3/NiO compositions and resulting $Li_xNi_{1-x}O$ solid solutions, and on gas evolution by Li_2CO_3 decompositions. While specific pore volume due to mass-to-void transformation increases with lithium carbonate content of the mixture, at high lithium content specific pore volume attributable to gas evolution decreases with Li_2CO_3 content, as the gas can escape from the high porous plaque, without formation of microporosity.

REFERENCES

1. PIGEAUD, A., MARU, H. C., PAETSCH, L., DOYON, J. & BERNARD, R., Recent developments in porous electrodes for molten carbonate fuel cells. In *Proceedings of the Symposium on Porous Electrodes: Theory and Practice*, ed. H. C. Maru, T. Katan & M. G. Klein. The Electrochemical Society, Inc., Pennington, NJ, 1984, pp. 234–259.
2. MINH, N. Q., Technological status of nickel oxide cathodes in molten carbonate fuel cells—a review. *J. Power Source*, **24** (1988) 1–19.
3. HATOH, K., NIIKURA, J., YASUMOTO, E. & GAMO, T., High lithium content of $Li_xNi_{1-x}O$ ($0 < x < 0.5$) for molten carbonate fuel cell cathode. *Denki Kagaku*, **64** (1996) 825–830.
4. SELMAN, J. R. & MARIANOWSKI, L. G., *Molten Salt Technology*, ed. D. G. Lovering. Plenum Press, New York, 1982, p. 323.
5. BAUMGARTNER, C. E. & ZARNOCH, K. P., Fabrication and characterization of porous lithium-doped nickel oxide cathodes for use in molten carbonate fuel cells. *Am. Ceram. Soc. Bull.*, **64** (1985) 593–597.
6. MANDARAZNY, F. N., BARTA, R. W., DEGAN, L. J., GRUBER, A., MARIANOWSKI, L. C., OSTHOFF, R. C. & REINSTROM, R. M., Development of molten carbonate fuel cells power plant. General Electric Company, Progress Report 1 February–30 April 1981, DOE/ET/17019-5, pp. 57–63.
7. ANTOLINI, E., LEONINI, M., MASSAROTTI, V., MARINI, A., BERBENNI, V. & CAPSONI, D., On the role of lithium carbonate in the preparation of doped nickel oxide cathodes for molten carbonate fuel cells. *Solid State Ionics*, **39** (1990) 251–261.
8. ANTOLINI, E., Sintering of $Li_xNi_{1-x}O$ solid solutions at 1200°C. *J. Mater. Sci.*, **27** (1992) 3335–3340.
9. ANTOLINI, E. & GIORDANI, M., Effect of lithium carbonate on the densification of $Li_xNi_{1-x}O$ solid solutions at temperatures up to 900°C. *Mater. Lett.*, **12** (1991) 117–122.
10. ANTOLINI, E., Formation of $Li_xNi_{1-x}O$ solid solution from Ni/Li_2CO_3 mixtures. *Mater. Lett.*, **16** (1993) 286–290.
11. MARINI, A., BERBENNI, V., MASSAROTTI, V., FLOR, G., RICCARDI, R. & LEONINI, M., Solid-state reaction study on the system Ni/Li_2CO_3. *Solid State Ionics*, **32/33** (1989) 398–408.
12. PICKERING, I. J., LEWANDOWSKI, J. T., JACOBSON, A. J. & GOLDSTONE, J. A., A neutron powder diffraction study of the ordering in $Li_xNi_{1-x}O$. *Solid State Ionics*, **53/56** (1992) 405–412.